

Mid-Infrared Selection of Brown Dwarfs and High-Redshift Quasars

Daniel Stern¹, J. Davy Kirkpatrick², Lori E. Allen³, Chao Bian⁴, Andrew Blain⁴, Kate Brand⁵, Mark Brodwin¹, Michael J. I. Brown⁶, Richard Cool⁷, Vandana Desai⁴, Arjun Dey⁸, Peter Eisenhardt¹, Anthony Gonzalez⁹, Buell T. Jannuzi⁸, Karin Menendez-Delmestre⁴, Howard A. Smith³, B. T. Soifer^{4,10}, Glenn P. Tiede¹¹ & E. Wright¹²

ABSTRACT

We discuss color selection of rare objects in a wide-field, multiband survey spanning from the optical to the mid-infrared. Simple color criteria simultaneously identify and distinguish two of the most sought after astrophysical sources: the coolest brown dwarfs and the most distant quasars. We present spectroscopically-confirmed examples of each class identified in the IRAC Shallow Survey of the Boötes field of the NOAO Deep Wide-Field Survey. ISS J142950.9+333012 is a T4.5 brown dwarf at a distance of approximately 42 pc, and ISS J142738.5+331242 is a radio-loud quasar at redshift $z = 6.12$. Our selection criteria identify a total of four candidates over 8 square degrees of the Boötes field. The other two candidates are both confirmed $5.5 < z < 6$ quasars, previously reported by Cool et al. (2006). We discuss the implications of these discoveries and conclude that there are excellent prospects for extending such searches to cooler brown dwarfs and higher redshift quasars.

¹Jet Propulsion Laboratory, California Institute of Technology, 4800 Oak Grove Dr., Mail Stop 169-506, Pasadena, CA 91109 [e-mail: stern@zwozkinder.jpl.nasa.gov]

²Infrared Processing and Analysis Center, California Institute of Technology, Pasadena, CA 91125

³Harvard-Smithsonian Center for Astrophysics, 60 Garden St., Cambridge, MA 02138

⁴Division of Physics, Math, and Astronomy, California Institute of Technology, Pasadena, CA 91125

⁵Space Telescope Science Institute, 3700 San Martin Dr., Baltimore, MD 21218

⁶Princeton University Observatory, Peyton Hall, Princeton University, Princeton, NJ 08544

⁷Steward Observatory, University of Arizona, 933 N. Cherry Ave., Tucson, AZ 85721

⁸National Optical Astronomy Observatory, 950 N. Cherry Ave., Tucson, AZ 85719

⁹Department of Astronomy, University of Florida, Gainesville, FL 32611

¹⁰*Spitzer* Science Center, California Institute of Technology, Pasadena, CA 91125

¹¹Department of Physics and Astronomy, Bowling Green State University, Bowling Green, OH 43403

¹²Department of Physics and Astronomy, University of California at Los Angeles, Los Angeles, CA 90095

Subject headings: surveys — stars: brown dwarfs — quasars: high-redshift — stars: individual (ISS J142950.9+333012) — quasars: individual (ISS J142738.5+331242)

1. Introduction

Wide-area surveys are one of the most powerful tools for observational astronomy, and have led to discoveries ranging from Earth-crossing asteroids to the most distant quasars. Historically, when technology allows a wavelength regime to be newly probed, either in terms of sensitivity or area, one of the first tasks is a large, shallow survey to see what astrophysical phenomena lurk in the uncovered territory. In recent years, major advances from this line of research include the discovery of the coolest Galactic stars by the Two Micron All Sky Survey (2MASS), ultraluminous infrared galaxies by the *Infrared Astronomical Satellite*, the most distant quasars by the Sloan Digital Sky Survey (SDSS), and the power spectrum of the cosmic microwave background, first by the *Cosmic Background Explorer* and later refined by the *Wilkinson Microwave Anisotropy Probe*. Such fundamental scientific discoveries have been a major incentive and reward for NASA’s Explorer program and other large projects. The pace of scientific discovery relies on such programs continuing.

The mid-infrared regime has been made newly accessible by the launch of the *Spitzer Space Telescope* (Werner et al. 2004). At its least competitive, shortest waveband, $3.6\mu\text{m}$, *Spitzer* is still more than five orders of magnitude more efficient than the largest ground-based observatories for areal surveys. For the longest wavebands, ground-based observations are simply not possible. Even compared to previous space-based missions, *Spitzer* offers several orders of magnitude increase in mapping efficiency.

Thus inspired, we have undertaken a shallow, wide-area 3.6 to $8.0\mu\text{m}$ survey with *Spitzer*, summarized in §2. We discuss two of the rare, interesting astronomical sources which are ideally suited to selection by combining deep optical data with shallow mid-infrared data: the coolest Galactic brown dwarfs and the most distant quasars. The former, of course, are not actually rare in the cosmos; their faint optical magnitudes merely delayed their discovery until recent years and continue to make them “rare” in terms of known, spectroscopically-confirmed examples. Section 3 discusses the selection criteria used to identify such sources and §4 describes our spectroscopic observations which confirmed both a cool brown dwarf (spectral class T4.5) and a high-redshift ($z = 6.12$) quasar. The implications for these discoveries are described in §4, and §5 summarizes the results and discusses future prospects. Throughout we adopt a $(\Omega_m, \Omega_\Lambda) = (0.3, 0.7)$ flat cosmology and $H_0 = 70\text{ km s}^{-1}\text{ Mpc}^{-1}$. Unless otherwise stated, all magnitudes are quoted in the Vega system.

2. Multiwavelength Surveys of Boötes

The Boötes field is a 9 deg^2 field which has been the target of deep observations across the electromagnetic spectrum. Boötes was initially selected as the North Galactic field of the NOAO Deep Wide-Field Survey (NDWFS; Jannuzi & Dey 1999), which obtained deep optical (B_WRI) and moderately-deep near-infrared (K_s) images across the entire field.¹³ These images reach approximate 5σ point source depths of $B_W = 27.1$, $R = 26.1$, $I = 25.4$ (B. Jannuzi et al., in prep.) and $K_s = 19.0$ (A. Dey et al., in prep.). Subsequently, the field has been observed at X-ray energies with the *Chandra X-Ray Observatory* (Murray et al. 2005), with a z' filter using the Bok 2.3m telescope at Kitt Peak (R. Cool in prep.), more deeply in the near-infrared (JK_s) as part of the FLAMINGOS Extragalactic Survey (FLAMEX; Elston et al. 2006), in the infrared with the *Spitzer Space Telescope* (Eisenhardt et al. 2004; Papovich et al. 2004), and at radio frequencies using the Westerbork Synthesis Radio Telescope (1.4 GHz; de Vries et al. 2002) and the Very Large Array (325 MHz; S. Croft et al., in prep.). Approximately 20,000 spectroscopic redshifts in the Boötes field have been obtained by the AGN and Galaxy Evolution Survey (AGES; C. Kochanek et al., in prep.) and Brodwin et al. (2006) reports on nearly 200,000 photometric redshifts in this field.

The mid-infrared imaging of Boötes is central to this paper. As part of a guaranteed-time observation program, 8 deg^2 of the field was imaged with the Infrared Array Camera (IRAC; Fazio et al. 2004) at 3.6 to $8 \mu\text{m}$. Eisenhardt et al. (2004) presents the survey design, reduction, calibration, and initial results. The survey, called the IRAC Shallow Survey, identifies $\approx 270,000$, 200,000, 27,000, and 26,000 sources brighter than 5σ Vega magnitude limits of 18.4, 17.7, 15.5, and 14.8 at 3.6, 4.5, 5.8, and $8.0 \mu\text{m}$, respectively, where IRAC magnitudes are measured in $6''$ diameter apertures and corrected to total magnitudes assuming sources are unresolved at the $1''.66 - 1''.98$ resolution of IRAC.

3. Mid-Infrared Selection of Rare Sources

Two core science goals of the IRAC Shallow Survey are the identification of the coolest stars and the identification of the most distant quasars. Both are optically-faint sources that are difficult to find, but are highly sought after for their astrophysical significance. Brown dwarfs probe the stellar-to-planetary link (e.g., Kirkpatrick 2005), while the highest redshift quasars probe the conditions of the early universe and the onset of cosmic reionization (e.g., Fan et al. 2006). Currently, there are less than 100 T-type brown dwarfs known and only ten quasars at $z > 6$. Both brown dwarfs and the most distant quasars are substantially brighter at mid-infrared wavelengths than at optical wavelengths. Therefore, wide-area, shallow, infrared surveys are ideally suited to identifying

¹³The third data release is publicly available at <http://www.archive.noao.edu/ndwfs>. The optical filter specifications are B_W ($\lambda_c = 4111 \text{ \AA}$, FWHM = 1275 \AA), R ($\lambda_c = 6514 \text{ \AA}$, FWHM = 1511 \AA), and I ($\lambda_c = 8205 \text{ \AA}$, FWHM = 1915 \AA). The R and I filters are part of the Harris filter set and the photometry was calibrated to match the Cousins system. The near-infrared filter conforms to the standard filter set.

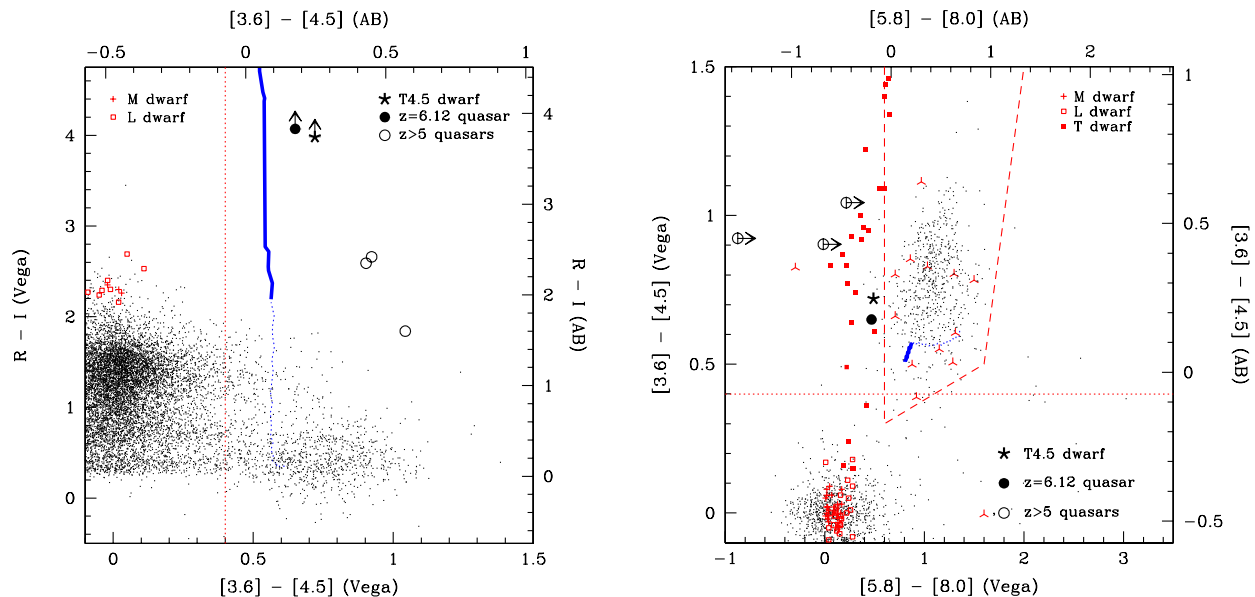


Fig. 1.— Color-color diagrams for unresolved sources in the Boötes field. As indicated, the asterisk refers to ISS J142950.9+333012 (T4.5 brown dwarf), the filled circle refers to ISS J142738.5+331242 ($z = 6.12$ quasar), and the open circles refer to Boötes field $5 < z < 6$ quasars from Cool et al. (2006). The dashed line in the right panel illustrates the empirically determined wedge largely populated by luminous, unobscured AGN (Stern et al. 2005). The dotted line illustrates the selection criteria employed in Cool et al. (2006) to identify luminous AGN which are too faint to be detected in all IRAC channels, $[3.6] - [4.5] > 0.4$. Dots illustrate typical colors of sources which are unresolved in the I band (starity index ≥ 0.8). In the left panel, sources with $18 < I < 20$ and $\geq 5\sigma$ detections in $[3.6]$ and $[4.5]$ are plotted. In the right panel, sources with $10 < I < 20$ and $\geq 5\sigma$ detections in all four IRAC passbands are plotted. Photometry of M, L, and T dwarfs from Dahn et al. (2002; optical) and Patten et al. (2006; IRAC) are plotted in red, as indicated. SDSS quasars at $z \approx 6$ are plotted as inverted-Y’s (Jiang et al. 2006). Quasars and typical stars are clearly separated on the basis of their mid-infrared colors. The blue line illustrates the colors of the SDSS quasar template from Richards et al. (2006) for $3 \leq z \leq 7$, subject to the Madau (1995) formulation for the opacity of the intergalactic medium as a function of redshift. The line becomes thicker for $z \geq 5.5$.

samples of both types of sources.

Brown dwarfs have red colors due to their cool temperatures. At mid-infrared wavelengths the spectra of *most* stars generally follow a Rayleigh-Jeans tail, giving them mid-infrared Vega colors near zero. For cooler stars and brown dwarfs, however, the presence of deep molecular absorptions results in very different emergent spectra (Kirkpatrick 2005). Specifically, the fundamental bands of CH_4 and CO between 3 and $5 \mu\text{m}$ (Oppenheimer et al. 1998; Rayner & Vacca 2005) and additional bands of H_2O , CH_4 , and NH_3 between 5 and $12 \mu\text{m}$ (Roellig et al. 2004) dramatically recarve the spectral energy distributions (SEDs) of these objects and give them unique IRAC colors (Patten

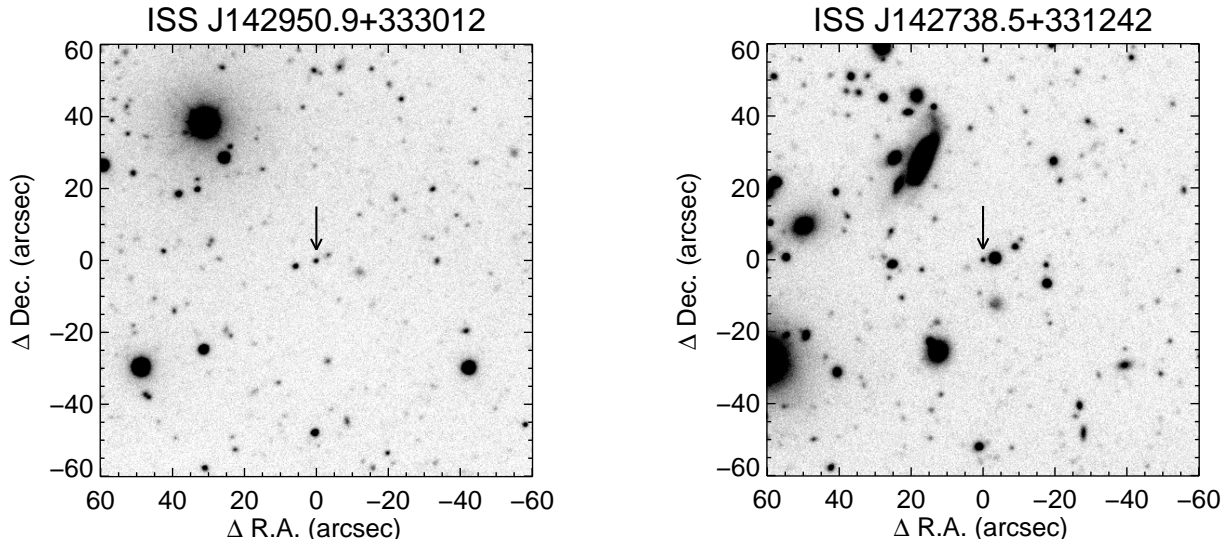


Fig. 2.— Finding charts for ISS J142950.9+333012 (T4.5 brown dwarf) and ISS J142738.5+331242 ($z = 6.12$ quasar) from the NDWFS I -band imaging. The fields are $2' \times 2'$, centered on the targets. North is at the top, and east is to the left.

et al. 2006). Shortward of $3 \mu\text{m}$, H_2O bands in L and T dwarfs (and CH_4 bands in T dwarfs only) cause deep depressions in the near-infrared spectra (e.g., McLean et al. 2003), and pressure-broadened Na I and K I resonance doublets suppress much of the flux below $1 \mu\text{m}$ (Kirkpatrick et al. 1999; Burgasser et al. 2003a), making brown dwarfs extremely faint in the optical. Specifically, the colors of known brown dwarfs later than type mid-T are $R - I > 3.5$ (Kirkpatrick et al. 1999; Dahn et al. 2002), $0.7 < [3.6] - [4.5] < 2$, and $0 < [5.8] - [8.0] < 0.8$ (Patten et al. 2006).

High-redshift quasars have red colors primarily due to absorption by foreground neutral hydrogen in the intergalactic medium which strongly suppresses the intrinsic UV emission of these AGN. At the highest redshifts, $z \gtrsim 6$, very little flux is detectable below $\text{Ly}\alpha$, providing the highest redshift quasars with similar optical colors to cool stars. Longward of $\text{Ly}\alpha$, luminous quasars are well-approximated by a power law and are easily identified in mid-infrared color-color diagrams (e.g., Stern et al. 2005).

Therefore, both the coolest brown dwarfs and the highest redshift quasars should easily be identifiable by selecting unresolved sources with very red optical colors and relatively flat (in f_ν) mid-infrared SEDs. Fig. 1 illustrates these selection criteria for the Boötes field. Note that at the highest redshifts, $z > 7$, quasars drop out of the optical completely. Typical colors of optical (I -band) point sources are presented. These color-color plots clearly separate stars and quasars, at least for typical, hot stars and typical, moderate-redshift quasars: most stars have mid-infrared colors near zero, while quasars are distinguished by their redder mid-infrared colors. Three confirmed quasars in this field at $5.39 \leq z \leq 5.85$ identified by Cool et al. (2006) are indicated, as are twelve $z \approx 6$ quasars from the SDSS (Jiang et al. 2006). The IRAC color-color criteria empirically

determined by Stern et al. (2005) and Cool et al. (2006) to select luminous AGN are indicated. Additionally, the colors of M, L, and T dwarfs from Dahn et al. (2002) and Patten et al. (2006) are plotted. The thick solid line shows the expected colors of $3 \leq z \leq 7$ quasars, calculated using the Richards et al. (2006) SDSS quasar template subject to the Madau (1995) formulation for the opacity of the intergalactic medium as a function of redshift. As can be seen, the Ly α forest causes high-redshift quasars to become very red in $R - I$ at $z \gtrsim 5$, while the mid-infrared colors vary only slightly over this large redshift range. Cool stars and high-redshift quasars are identifiable from their red $R - I$ and $[3.6] - [4.5]$ colors. Longer-wavelength, $[5.8] - [8.0]$ colors can provide additional information, but require deeper data to obtain robust detections in these less-sensitive passbands.

As seen in Fig. 1, both brown dwarfs and high-redshift quasars should be easily identified using the simple (Vega-system) selection criteria of (i) $R - I \geq 2.5$, (ii) $[3.6] - [4.5] \geq 0.4$, and (iii) unresolved at I -band. To restrict the number of spurious sources identified in the catalogs, we also require (iv) $B_W - I \geq 2.5$. These constraints implicitly require robust detections (or robust non-detections) in the various bands. In particular, the I -band morphology criterion requires $I \lesssim 23$ for the NDWFS survey. According to the work of Patten et al. (2006), the IRAC color criterion eliminates sources hotter than spectral class T3. The Boötes $4.5\mu\text{m}$ catalog (ver. 1.3) identifies 30 candidates matching these selection criteria, which are trimmed to four robust candidates after visual inspection. The most common cause of a false positive is source blending. One source, ISS J142918.1+343731, appeared modestly robust after visually inspecting the ground-based imaging. However, the source resides near a $z > 1$ galaxy cluster identified by Eisenhardt et al. (2006). *Hubble Space Telescope* imaging of the cluster (GO 10836; P.I. S. Perlmutter) shows that the potential candidate is compact, but clearly resolved, and thus unlikely to be either a brown dwarf or a high-redshift quasar. Two of the final four candidates have already been spectroscopically confirmed as $5.5 < z < 6$ quasars by Cool et al. (2006). The remaining two were targeted spectroscopically during Spring 2006, as discussed next. Table 1 presents all four Boötes field candidates, in order of decreasing $3.6\mu\text{m}$ flux, and Fig. 2 presents finding charts for the two sources described in §4.

4. Spectroscopic Observations and Discussion

Initial spectroscopic follow-up of candidates was obtained with the Multi-Aperture Red Spectrometer (MARS; Barden et al. 2001) on the Mayall 4m telescope at Kitt Peak. MARS is an optical spectrograph which uses a high resistivity, p-channel Lawrence Berkeley National Laboratory CCD with little fringing and very high throughput at long wavelengths ($\lesssim 10,500 \text{ \AA}$). On the nights of UT 2006 March 24 – 26, we obtained spectra of red sources in the Boötes field using the $1''7$ wide long slit, OG550 order-sorting filter, and the VG8050 grism. Across much of the optical window, the instrument configuration provides resolution $R \approx 1100$ spectra, as measured from sky lines filling the slit. ISS J142950.9+333012 was observed for 1.5 hr on UT 2006 March

24, split into three dithered 1800 s exposures. ISS J142738.5+331242 was observed for 1 hr on UT 2006 March 25, split into three 1200 s exposures. The data were processed following standard optical, slit spectroscopy procedures. The nights were not photometric, but relative flux calibration of the spectra was achieved with observations of the spectrophotometric standards Feige 34 and PG 0823+546 (Massey & Gronwall 1990) obtained during the same observing run. The extracted, calibrated MARS spectra are presented in Figs. 3 and 5. The bright star $3''3$ east of ISS J142738.5+331242 made extraction of the fainter target challenging, resulting in systematic fluctuations of the background at the $1 \mu\text{Jy}$ level.

Near-infrared spectroscopy of ISS J142950.9+333012 was obtained with the cryogenic, cross-dispersed Near-Infrared Echelle Spectrograph (NIRSPEC; McLean et al. 1998) on the Keck II 10m telescope atop Mauna Kea. We first obtained J - and H -band spectroscopy on UT 2006 April 05. An AB nod sequence with a total on-source integration time of 200 s per grating setting was used. For both grating settings, the G2 V star GSPC P300-E from Colina & Bohlin (1997) was used for both telluric correction and flux calibration. An additional J -band spectrum was acquired on UT 2006 May 11. On this night a 300 s integration was taken both on-source and off-source, and the F0 star BD+66 1089 was acquired for telluric correction and flux calibration. Fig. 4 presents the combined near-infrared spectrum.

4.1. ISS J142950.9+333012: Mid-T Brown Dwarf

The spectrum of ISS J142950.9+333012 shows the classic signatures of a T dwarf. The optical spectrum in Fig. 3 shows a sharp rise to the longest wavelengths, indicative of a cool temperature and strong absorption by the pressure-broadened wings of K I (and to some extent Na I). Even more telling are the J - and H -band spectra in Fig. 4 that show strong CH_4 and H_2O absorption, the former of which is the hallmark of spectral class T.

As this object has both optical and near-infrared spectra, we can classify on both the optical and near-infrared classification schemes. The optical typing of T dwarfs is somewhat crude because the $\leq 1\mu\text{m}$ spectra show less variation than at longer wavelengths. Nonetheless, Burgasser et al. (2003a) have established standards for classes T2, T5, T6, and T8. In the $6000 - 10000 \text{ \AA}$ range the best diagnostic is the 9300 \AA band of H_2O . Unfortunately our MARS spectrum has not been telluric corrected so the depth of this water feature will be influenced by both the earth's atmosphere as well as the atmosphere of the brown dwarf itself. This feature in ISS J142950.9+333012 is not as deep as in the spectrum of a T8, so the true spectral type must be earlier than that. Comparisons with the T2, T5, and T6 standards obtained with Keck (Burgasser et al. 2003a) show that the overall slope most resembles that of the T5. Given the coarseness of classification in this wavelength regime, we can assign only a crude optical spectral type of $\text{T}5 \pm 2$.

In the near-infrared the situation is much improved. In this wavelength regime there is a full set of standards for each spectral subtype from T0 to T8 (Burgasser et al. 2006). Using Keck

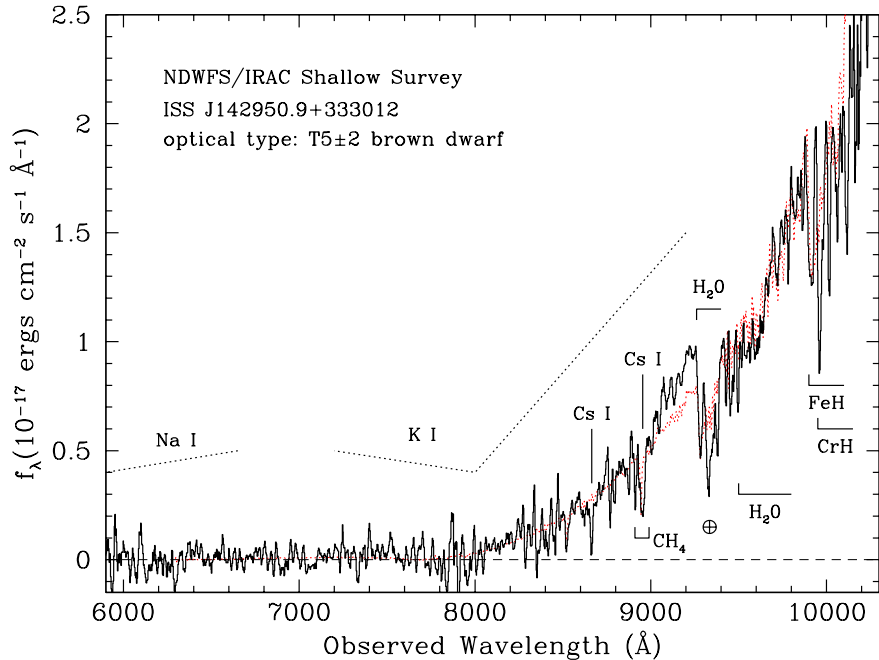


Fig. 3.— Optical spectrum of ISS J142950.9+333012, optically classified as a T5±2 brown dwarf, obtained with the MARS spectrograph on KPNO 4m telescope. The relative flux calibration was determined from observations of standard stars from the same observing runs with the same instrumental configurations. The spectrophotometric scale was estimated from the imaging. The dotted spectrum shows 2MASS J055919.14–140448.8, classified as a T5 brown dwarf at optical wavelengths (Burgasser et al. 2003a).

NIRSPEC spectra from McLean et al. (2003) of the Burgasser et al. (2006) standards, we find that the individual J -band spectra best match a type intermediate between T4 and T5. A similar fit to the H -band data alone gives the identical result. These results point to a solid near-infrared spectral type of T4.5.

Shown in Figs. 3 - 4 are comparisons of the spectra of ISS J142950.9+333012 and 2MASS J0559–1404, which is the optical T5 standard and typed as T4.5 on the Burgasser et al. (2006) near-infrared scheme. (That is, 2MASS J0559–1404 has the same type as ISS J142950.9+333012 in both wavelength regimes.) Note the similarities between the two spectra. 2MASS J0559–1404 has a well measured trigonometric parallax of 97.7 ± 1.3 mas (Dahn et al. 2002) and an absolute magnitude of $M_J = 13.75 \pm 0.04$, which allows us to estimate a distance to ISS J142950.9+333012 of 42 pc, assuming both T dwarfs are single. However, 2MASS J0559–1404 is the most overluminous object in the early-/mid-T “hump” on the Hertzsprung-Russell diagram (see Vrba et al. 2004; Golimoski et al. 2004), leading some researchers to believe that it might be a close, equal-magnitude double despite all current evidence to the contrary (Burgasser et al. 2003b; Gelino & Kulkarni 2005; Liu et al.

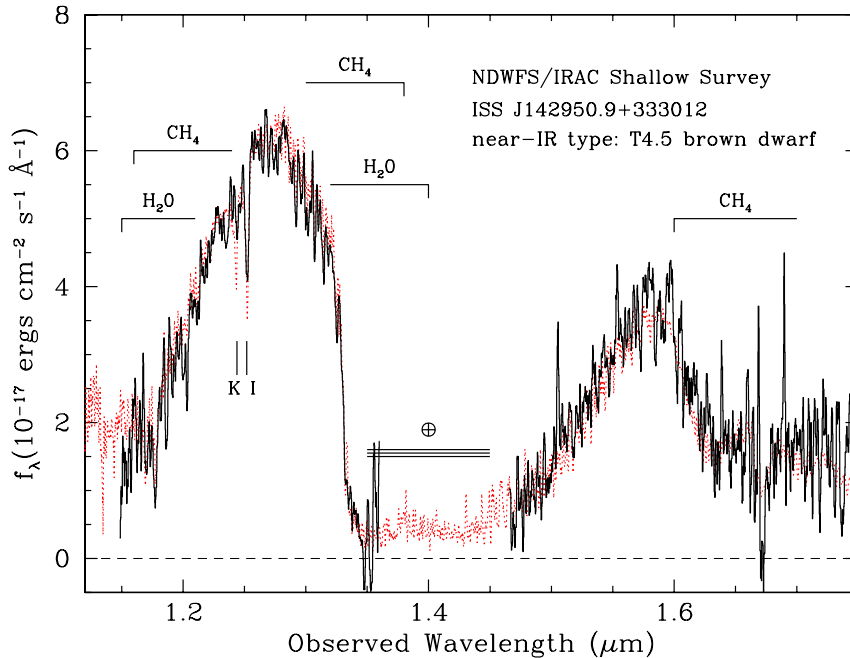


Fig. 4.— Near-infrared spectrum of ISS J142950.9+333012 obtained with the NIRSPEC spectrograph on the Keck II telescope, classified as a Galactic T4.5 brown dwarf from these data. The relative flux calibration was determined from observations of standard stars from the same observing runs with the same instrumental configurations. The spectrophotometric scale was estimated from the imaging. The dotted line shows the infrared spectrum of 2MASS J0559–1404, classified as a T4.5 brown dwarf in the near-infrared (McLean et al. 2003).

2006). Correcting for this possibility, we find that ISS J142950.9+333012 might be as close as 30 pc. No other optically classified T dwarfs are known of spectral type T5; the only other T dwarf with a measured trigonometric parallax and near-infrared type of T4.5 is SDSS J020742.48+000056.2. The parallax measurement of 34.85 ± 9.87 mas for SDSS J0207+0000 (Vrba et al. 2004) implies $M_J = 14.51 \pm 0.64$, which is very uncertain but lends some weak support to the closer distance estimate for ISS J142950.9+333012.

The first images to detect the brown dwarf were the NDWFS *I*-band observations obtained on UT 2000 April 28, 3.7 yr prior to the IRAC imaging. Comparing ten nearby sources detected in both the *I*-band and $3.6\mu\text{m}$ observations, ISS J142950.9+333012 has a detected proper motion of $0''.1 \pm 0''.03 \text{ yr}^{-1}$, in a southerly direction. This is comparable in amplitude to the expected reflex solar motion for a source at ≈ 40 pc. Interestingly, the star $5''.7$ east of the brown dwarf shows a higher proper motion, $\mu = 0''.3 \pm 0''.03 \text{ yr}^{-1}$ in the NW direction. The colors of this $R = 22.3$ star (ISS J142951.3+333010) are relatively blue, $B_W - R = 0.6$, $R - I = 0.6$, suggesting a relatively hot white dwarf at a distance of several hundred pc, moving at several hundred km sec^{-1} .

The $4.5\mu\text{m}$ flux of the brown dwarf is 2.7 mag brighter than the survey limit (i.e., $V/V_{\text{max}} = 0.024$), whereas the I magnitude is only 0.9 mag above the limit ($V/V_{\text{max}} = 0.3$). This suggests that the $I < 23$ requirement imposed to provide robust morphological selection of unresolved sources is a significant limiting factor. We estimate that our selection criteria restrict our sensitivity to brown dwarfs of spectral type T3 to T6. The former limit comes from the IRAC color criterion (Patten et al. 2006). The latter limit comes from available data (J.D. Kirkpatrick et al., in prep.) suggesting that I -band flux drops dramatically for spectral types cooler than T6. From Vrba et al. (2004) and Golimoski et al. (2004), the range T3 to T6 corresponds very roughly to $T_{\text{eff}} = 1500$ to 1100 K. Using a model which forms brown dwarfs at a constant rate over 10 Gyr with power law mass functions of index 0.4 to 1.3 (Reid, Gizis, & Hawley 2002) and the theoretical models of Burrows, Sudarsky, & Lunine (2003) which give luminosities and T_{eff} as a function of brown dwarf mass and age, we expect 3 – 5 brown dwarfs in the IRAC shallow survey to meet our selection criteria. Intriguingly, there should be a similar number of dwarfs with $T_{\text{eff}} < 750$ K above the [4.5] flux limit, although our $I < 23$ requirement would exclude them from the present sample.

Given our desire to understand more fully the physical nature of the L/T transition, the newly discovered T4.5 brown dwarf can serve as another probe of the overluminosity of the early-/mid-T hump. Its magnitudes of $J = 16.88$ and $K_s = 16.99$ make it a difficult but not impossible target for a dedicated near-infrared parallax program such as the on-going one at the US Naval Observatory in Flagstaff (Vrba et al. 2004). More importantly, ISS J142950.9+333012 is the first example of a field T dwarf selected by mid-infrared photometry supplemented by other ground-based optical and near-infrared data. This implies that a very similar selection technique to be employed by the *Wide-Field Infrared Survey Explorer* (*WISE*; Eisenhardt & Wright 2003), planned for launch in 2009, is sound and will be capable of discovering other T dwarfs, and hopefully cooler Y dwarfs (Kirkpatrick 2003). *WISE* will sample hundreds of times more volume than the IRAC Shallow Survey in bands similar to [3.6] and [4.5], and should reveal whether there are brown dwarfs closer to the Sun than Proxima Centauri.

4.2. ISS J142738.5+331242: $z = 6.12$ Quasar

The spectrum of ISS J142738.5+331242 (Fig. 5) clearly shows the strong $\text{Ly}\alpha$ emission and strong $\text{Ly}\alpha$ decrement of a $z \geq 6$ quasar. At a redshift of $z = 6.12$, ISS J142738.5+331242 is emitting when the universe was 0.89 Gyr old, or only 7% of its current age. This is the tenth $z \geq 6$ quasar identified to date, with the prior nine identified by the Sloan Digital Sky Survey (SDSS; Fan et al. 2006). ISS J142738.5+331242 was identified independently by McGreer et al. (2006) using different selection criteria. Two characteristics separate ISS J142738.5+331242 from the other nine $z \geq 6$ quasars known. First, while the other nine were identified from 6550 deg^2 of the wide-area, shallow SDSS optical survey with J -band follow-up, ISS J142738.5+331242 was identified in a more sensitive, multi-wavelength survey of only 8 deg^2 . Consequently, this is the least luminous quasar known at $z \approx 6$. Secondly, the Faint Images of the Radio Sky at Twenty-cm survey (FIRST; Becker,

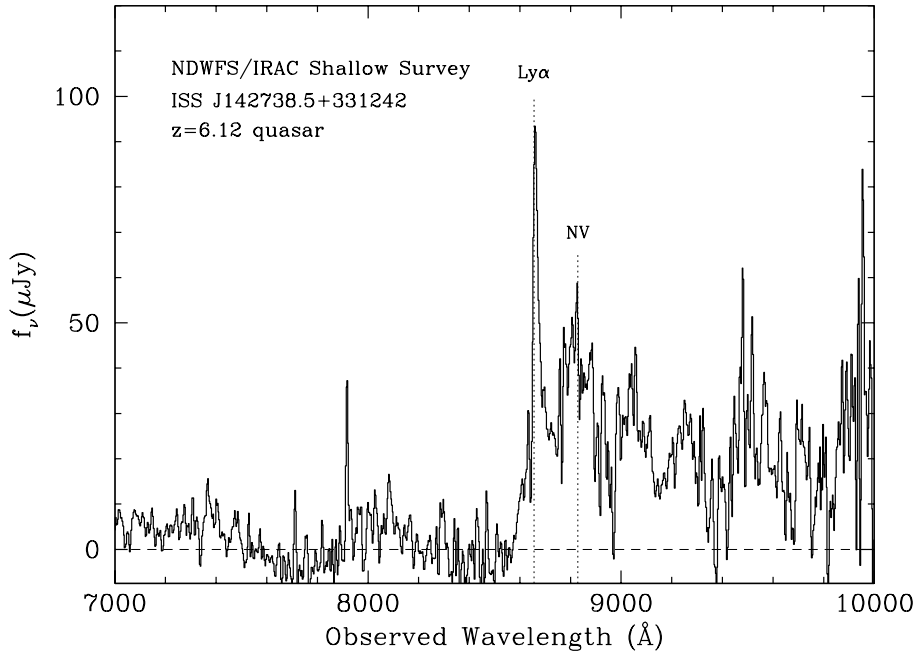


Fig. 5.— Spectrum of ISS J142738.5+331242, a quasar at $z = 6.12$, obtained with the MARS spectrograph on the Kitt Peak 4m Mayall telescope. The relative flux calibration was determined from observations of standard stars from the same observing run with the same instrumental configuration. As the nights were not photometric, the spectrophotometric scale has been estimated from the imaging.

White, & Helfand 1995) identifies a source with an integrated flux of 1.03 mJy within 1 arcsec of the quasar coordinates. ISS J142738.5+331242 is thus the only $z \geq 6$ mJy-radio source currently known.

The evolution of the fraction of quasars which are radio loud, and, in fact, the definition and very existence of such a dichotomy, has been the subject of substantial literature. Some researchers prefer a definition based on the radio-optical ratio R_{ro} of the specific fluxes at rest-frame 6 cm (5 GHz) and 4400 Å (Kellerman et al. 1989). The other common definition divides the populations at some rest-frame radio luminosity; e.g., Gregg et al. (1996) uses a cutoff value for the 1.4 GHz specific luminosity, $L_{1.4 \text{ GHz}} = 10^{32.5} h_{50}^{-2} \text{ ergs s}^{-1} \text{ Hz}^{-1}$ to separate radio loud and radio quiet sources.¹⁴ The latter definition is immune to obscuration from dust, and, as argued by Peacock, Miller, & Longair (1986) and Miller, Peacock, & Mead (1990), is the more physically meaningful definition. Based on radio observations of all $z > 4$ quasars known as of mid-1999 and using the radio luminosity definition, Stern et al. (2000) found that approximately 12% of quasars are radio

¹⁴An Einstein-de Sitter cosmology is assumed.

loud, with no evidence of this fraction depending on either redshift (for $2 \lesssim z \lesssim 5$) or optical luminosity (for $-25 \gtrsim M_B \gtrsim -28$). For a typical radio spectral index $\alpha = -0.5$ and an Einstein-de Sitter cosmology for comparison with previous literature, ISS J142738.5+331242 has a radio luminosity of $L_{1.4 \text{ GHz}} = 1.33 \times 10^{33} h_{50}^{-2} \text{ ergs s}^{-1} \text{ Hz}^{-1}$, classifying it as radio loud. McGreer et al. (2006) show that this source is still classified as radio loud based on a radio-optical ratio definition. ISS J142738.5+331242 is thus the most distant radio-loud quasar known.

ISS J142738.5+331242 is only slightly fainter in luminosity than the $z \geq 6$ SDSS quasars, so we consider all ten $z > 6$ quasars as a single sample, deferring issues of the likelihood of our having found such a source in our drastically smaller survey (discussed next). The implication is that the radio loud fraction remains near 10% out to $z \approx 6.5$. Conventional wisdom and morphological studies suggest that luminous, radio loud AGN are preferentially identified with early-type galaxies (e.g., McLure et al. 1999). Theory can explain the trend, since early-type galaxies are likely the products of major mergers and two coalescing supermassive black holes appear necessary to create black holes of sufficient spin to generate highly collimated jets and powerful radio sources (e.g., Wilson & Colbert 1995). Assuming the radio loud – luminous host galaxy relation remains robust at high redshift, the apparent discovery that $\approx 10\%$ of quasars are radio loud out to the highest redshifts probed has interesting implications for the formation epoch of massive galaxies. In hierarchical models of galaxy formation, late-type (less massive) systems form first and mergers are required to form the early-type (more massive) systems. Eventually, therefore, one expects the radio-loud fraction of AGNs to fall precipitously with redshift. Our results show this epoch lies beyond $z \approx 6$, providing further evidence for an early formation epoch for massive galaxies. The stellar masses of *i*-dropout galaxies in the Great Observatories Origins Deep Survey (Giavalisco et al. 2004) leads to a similar conclusion from a very different data set and line of argument (Yan et al. 2005, 2006; Eyles et al. 2006).

How likely was the discovery of this distant quasar in an 8 deg^2 field? Interpolating the K_s and $3.6 \mu\text{m}$ photometry for ISS J142738.5+331242 implies $m_{\text{AB}}[(1+z)4400\text{\AA}] \approx 19.6$, or $M_{\text{AB}}(4400) = -27.2$. For a typical quasar optical spectral index, the conversion between AB-system $M_{\text{AB}}(4400)$ and Vega-system M_B is $M_B = M_{\text{AB}}(4400) + 0.12$ (e.g., Stern et al. 2000), implying $M_B = -27.1$ for ISS J142738.5+331242. Our *J*-band photometry implies a continuum flux density of $\approx 18 \mu\text{Jy}$ at $1 \mu\text{m}$, or a rest-frame UV luminosity of $M(1450) = -26.0$, making this source fainter than any of the $z \approx 6$ quasars identified by the SDSS (Fan et al. 2006). McGreer et al. (2006) found a slightly brighter absolute magnitude, $M(1450) = -26.4$, likely due to their alternate methodology whereby a quasar template fit to the IRAC data was used to derive the rest-frame UV luminosities.

We estimate the number of high-redshift quasars expected from our selection criteria using the Fan et al. (2004) high-redshift quasar luminosity function, derived from the SDSS. We approximate high-redshift quasar spectra as step functions, with zero flux below redshifted $\text{Ly}\alpha$ and a flat SED (in f_ν) redward of $\text{Ly}\alpha$, and we approximate the NDWFS *I*-band filter as a tophat function. Our selection criteria restrict our sensitivity to quasars at $5.5 \lesssim z \lesssim 6.5$. The lower redshift limit comes

from the $R - I$ color requirement, determined from the Richards et al. (2006) model discussed in §3; indeed, the $z = 5.39$ quasar identified by Cool et al. (2006) is too blue in $R - I$ to meet our selection criteria (Fig. 1). The upper redshift limit corresponds to Ly α shifting out of the I -band filter. The Fan et al. (2004) luminosity function predicts 3.3 quasars at $5.5 < z < 6.5$ with $I < 23$ in our 8 deg² survey. This prediction exactly matches the current results, though, notably, the faintest of the high-redshift Boötes quasars has $I = 22.0$, suggesting that more quasars remain to be discovered with $22 < I < 23$ and that the faint end slope of the high-redshift quasar luminosity function is steeper than currently assumed. Of the 3.3 quasars predicted at $5.5 < z < 6.5$, only 0.3 are expected to be at $z > 6$, or, for 12% of quasars being radio-loud (Stern et al. 2000), we only had a 4% chance of identifying a $z > 6$ radio-loud quasar in this survey. While it is premature to make strong claims from this small sample, our results imply possible rapid evolution in the faint end of the quasar luminosity function and in the radio loud fraction at high redshift.

5. Summary and Future Prospects

We report the discovery of the first mid-infrared selected field brown dwarf and the discovery of the most distant radio loud source known. Fig. 6 plots the observed SEDs of these two sources, with a model brown dwarf spectrum from Burrows, Sudarsky, & Hubeny (2006) and a model high-redshift quasar from Richards et al. (2006). Interestingly, despite nine orders of magnitude difference in luminosity distance, or nearly 20 orders of magnitude difference in luminosity, the broad-band optical colors, the broad-band mid-infrared colors, and the multi-wavelength brightnesses of these two extremely disparate sources are nearly identical. With only $B_W RI$ and IRAC photometry, there is no possibility to separate mid-T brown dwarfs and high-redshift quasars. As shown in Fig. 7, however, near-infrared photometry offers the possibility to separate the two source types. While quasars have red $J - K_s$ colors, the latest T dwarfs have blue near-infrared colors, $J - K_s \lesssim 0.5$.

We have presented simple color criteria which very efficiently identify astrophysically interesting sources. Using the Boötes 4.5 μ m-selected catalog, the criteria presented in §3 identify 30 potential candidates which were trimmed down to four robust candidates after visual inspection. The primary weakness of the criteria is that we have only found objects at the edge of current observations, not beyond them – e.g., ISS J142950.9+333012 is the among the 50 coldest brown dwarfs known and ISS J142738.5+331242 is the 6th most distant quasar known. To push to new territory such as Y dwarfs and $z > 7$ quasars will require modifying the selection criteria in §3, and, most likely, surveying more of the celestial sphere. In our current search, the $I \leq 23$ criterion imposed to ensure robust morphological selection of unresolved sources is the most restrictive requirement. Probing deeper would allow the detection of fainter sources, but to identify Y dwarfs and $z > 7$ quasars will likely require robust morphological information at longer wavelengths.

We consider the effects of relaxing the selection criteria identified in §3. If we retain the requirement $I \leq 23$ but drop the morphological requirement for a point source, we obtain 434 candidates. Going a magnitude more deeply in I -band, where NDWFS photometry is still robust

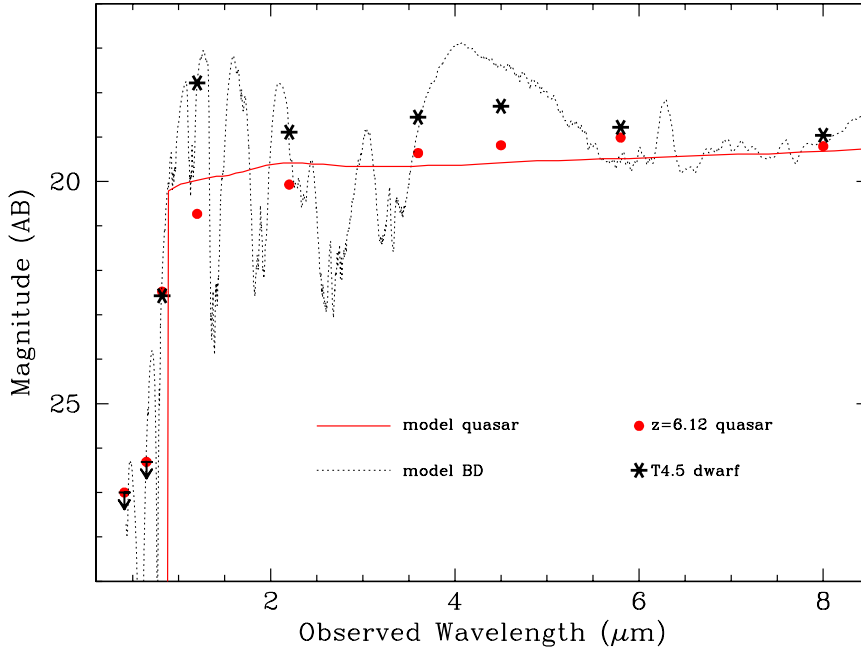


Fig. 6.— Spectral energy distributions of the two sources discussed in this paper, ISS J142950.9+333012, a T4.5 brown dwarf, and ISS J142738.5+331242, a $z = 6.12$ quasar. Based on broad-band photometry, the optical and IRAC properties of these two very different sources are nearly identical; only at near-infrared wavelengths do they differ significantly. The dotted line illustrates a model brown dwarf spectrum from Burrows et al. (2006) for $T_{\text{eff}} = 1000$ K, $g = 10^5 \text{ cm s}^{-2}$, solar metallicity, and a modal cloud particle size of $100 \mu\text{m}$. The solid line illustrates a model quasar at $z = 6.12$ from Richards et al. (2006), assuming no flux is detected below redshifted Ly α .

but star-galaxy morphological separation fails, nearly quadruples the number of candidates to 1598 sources. Galaxies at $z \gtrsim 1$ have red $R - I$ colors and IRAC $[3.6] - [4.5] \geq 0.4$ (e.g., see model tracks in Stern et al. 2005), thereby causing significant contamination. At $z \gtrsim 7$, quasars will fall out of the NDWFS I -band, so one might think that selecting optical dropouts with IRAC $[3.6] - [4.5] \geq 0.4$ would provide efficient criteria to identify the most distant quasars. Unfortunately, red galaxies are again a contaminant: there are nearly 10,000 sources in the Boötes field with $[3.6] - [4.5] \geq 0.4$ and no detection in the optical passbands. We are currently experimenting with various schemes to trim these large samples that arise when morphological criteria aren't available. One possibility, amenable to searching for cool dwarfs, is to search for sources with blue near-infrared colors (e.g., $J - K_s < 0.5$), but red colors in $[3.6] - [4.5]$. The former criterion should identify both hot and cold Galactic stars, while the latter criterion eliminates the hot stars. Since extragalactic sources are typically redder in $J - K_s$ (e.g., Fig. 7 in Elston et al. 2006), these criteria should identify T dwarfs (and colder) irrespective of morphology. Another solution would be to obtain better morphological measurements, as are available in the (smaller area) Extended Groth Strip

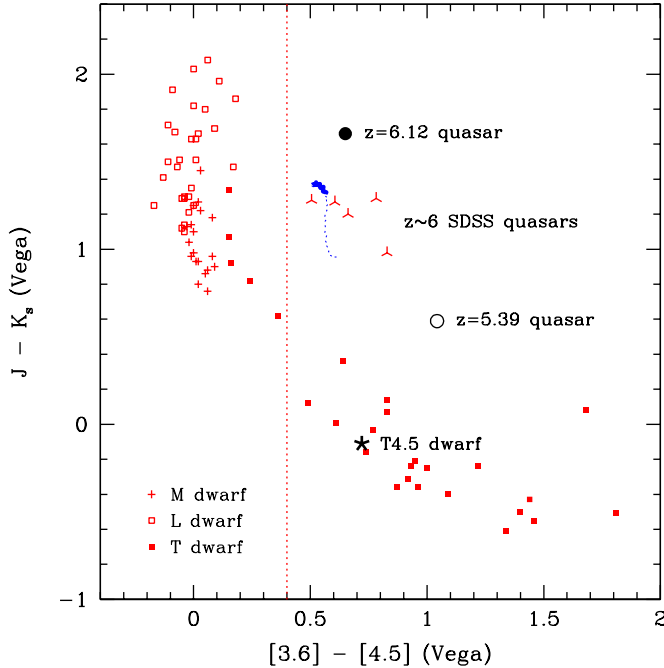


Fig. 7.— Color-color diagrams for cool stars and high-redshift quasars. Black symbols are for sources in the Boötes field: the asterisk refers to ISS J142950.9+333012 (T4.5 brown dwarf), the filled circle refers to ISS J142738.5+331242 ($z = 6.12$ quasar), and the open circle refers to the $z = 5.39$ quasar in Cool et al. (2006). The vertical dotted line illustrates the selection criteria employed in Cool et al. (2006) to identify luminous AGN, $[3.6] - [4.5] > 0.4$. Photometry of M, L, and T dwarfs from Patten et al. (2006) are plotted in red, as indicated. Photometry of $z \approx 6$ SDSS quasars from Jiang et al. (2006) are plotted as inverted-Y’s. The solid blue line illustrates the colors of the SDSS quasar template from Richards et al. (2006) for $3 \leq z \leq 7$, subject to the Madau (1995) formulation for the opacity of the intergalactic medium as a function of redshift (the line becomes thicker for $z \geq 5.5$). The vertical line separates high-redshift quasars and dwarfs later than T3 from the hotter dwarfs. The near-infrared $J - K_s$ color looks like a promising diagnostic to separate the coolest brown dwarfs from the high-redshift quasars.

and the COSMOS surveys, or should also be obtainable with the new generation of wide-field, near-infrared cameras.

Our observations illustrate some of the interesting sources identifiable from wide-area mid-infrared surveys. After *Spitzer* has depleted its cryogen, expected to occur in early- to mid-2009, wide-area 3.6 and 4.5 μm surveys are likely to be an emphasis for the observatory. Shortly thereafter, the launch of the *WISE* will provide full-sky, mid-infrared images. Such surveys, combined with the deep, complementary optical data expected from the Panoramic Survey Telescope and Rapid Response System (Pan-STARRS; Kaiser et al. 2005) and the Large Synoptic Survey Telescope (LSST; Tyson et al. 2005), should prove very valuable for studying both the nearest, coldest stars

and for identifying the most distant, luminous quasars. The former will enhance our knowledge of star formation and Galactic structure. The latter will probe the first cosmic structures, the history of the intergalactic medium, and literally expand the limits of human knowledge.

We thank Chris Kochanek and Steve Willner for useful comments on the manuscript. This work is based on observations made with the *Spitzer Space Telescope*, which is operated by the Jet Propulsion Laboratory, California Institute of Technology. Support was provided by NASA through an award issued by JPL/Caltech. This work also made use of images and/or data products provided by the NDWFS, which is supported by the National Optical Astronomy Observatory (NOAO). NOAO is operated by AURA, Inc., under a cooperative agreement with the National Science Foundation. AD and BJ are supported by NOAO. We thank the staff of KPNO and Keck for their expert assistance with our observations. Research has benefited from the M, L, and T dwarf compendium housed at <http://DwarfArchives.org>. The authors also wish to recognize and acknowledge the very significant cultural role and reverence that the summit of Mauna Kea has always had within the indigenous Hawaiian community; we are most fortunate to have the opportunity to conduct observations from this mountain.

REFERENCES

- Barden, S., Dey, A., Lynds, R., Reed, R., Ditsler, B., & Harmer, C. 2001, NOAO Newsletter, 67, 31
- Becker, R. H., White, R. L., & Helfand, D. J. 1995, ApJ, 450, 559
- Brodwin, M. et al. 2006, ApJ, in press (astro-ph/0607450)
- Burgasser, A. J., Geballe, T. R., Leggett, S. K., Kirkpatrick, J. D., & Golimowski, D. A. 2006, ApJ, 637, 1067
- Burgasser, A. J., Kirkpatrick, J. D., Liebert, J., & Burrows, A. 2003a, ApJ, 594, 510
- Burgasser, A. J., Kirkpatrick, J. D., Reid, I. N., Brown, M. E., Miskey, C. L., & Gizis, J. E. 2003b, ApJ, 586, 512
- Burrows, A., Sudarsky, D., & Hubeny, I. 2006, ApJ, 640, 1063
- Burrows, A., Sudarsky, D., & Lunine, J. I. 2003, ApJ, 596, 587
- Colina, L. & Bohlin, R. 1997, AJ, 113, 1138
- Cool, R. et al. 2006, AJ, 132, 823
- Dahn, C. C. et al. 2002, AJ, 124, 1170

- de Vries, W. H., Morganti, R., Röttgering, H. J. A., Vermeulen, R., van Breugel, W., Rengelink, R., & Jarvis, M. J. 2002, *AJ*, 123, 1784
- Eisenhardt, P. R. & Wright, E. L. 2003, *SPIE*, 4850, 1050
- Eisenhardt, P. R. et al. 2004, *ApJS*, 154, 48
- . 2006, *ApJ*, in prep.
- Elston, R. et al. 2006, *ApJ*, 639, 816
- Eyles, L., Bunker, A., Ellis, R., Lacy, M., Stanway, E., Stark, D., & Chiu, K. 2006, *MNRAS*, submitted (astro-ph/0607306)
- Fan, X. et al. 2004, *AJ*, 128, 515
- . 2006, *AJ*, 132, 117
- Fazio, G. G. et al. 2004, *ApJS*, 154, 10
- Gelino, C. R. & Kulkarni, S. R. 2005, *BAAS*, 207, #78.12
- Giavalisco, M. et al. 2004, *ApJ*, 600, L93
- Golimoski, D. A. et al. 2004, *ApJ*, 127, 3516
- Gregg, M. D., Becker, R. H., White, R. L., Helfand, D. J., McMahon, R. G., & Hook, I. M. 1996, *AJ*, 112, 407
- Jannuzi, B. T. & Dey, A. 1999, in *Photometric Redshifts and High-Redshift Galaxies*, ed. R. Weymann, L. Storrie-Lombardi, M. Sawicki, & R. Brunner, Vol. 191 (San Francisco: ASP Conference Series), 111
- Jiang, L. et al. 2006, *AJ*, in press (astro-ph/0608006)
- Kaiser, N. et al. 2005, *BAAS*, 270, #150.04
- Kellerman, K. I., Sramek, R., Schmidt, M., Shaffer, D. B., & Green, R. 1989, *AJ*, 98, 1195
- Kirkpatrick, J. D. 2003, *IAU Symposium*, 211, 497
- . 2005, *ARA&A*, 43, 195
- Kirkpatrick, J. D. et al. 1999, *ApJ*, 519, 802
- Liu, M. C., Leggett, S. K., Golimowski, D. A., Chiu, K., Fan, X., Geballe, T. R., Schneider, D. P., & Brinkmann, J. 2006, *ApJ*, in press (astro-ph/0605037)
- Madau, P. 1995, *ApJ*, 441, 18

- Massey, P. & Gronwall, C. 1990, *ApJ*, 358, 344
- McGreer, I. D., Becker, R. H., Helfand, D. J., & White, R. L. 2006, *ApJ*, submitted (astro-ph/0607278)
- McLean, I. S., McGovern, M. R., Burgasser, A. J., Kirkpatrick, J. D., Prato, L., & Kim, S. S. 2003, *ApJ*, 596, 561
- McLean, I. S. et al. 1998, *SPIE*, 3354, 566
- McLure, R. J., Kukula, M. J., Dunlop, J. S., Baum, S. A., O’Dea, C. P., & Hughes, D. H. 1999, *MNRAS*, 308, 377
- Miller, L., Peacock, J. A., & Mead, A. R. G. 1990, *MNRAS*, 244, 207
- Murray, S. S. et al. 2005, *ApJS*, 161, 1
- Oppenheimer, B. R., Kulkarni, S. R., Matthews, K., & van Kerkwijk, M. H. 1998, *ApJ*, 502, 932
- Papovich, C. et al. 2004, *ApJ*, 600, L111
- Patten, B. M. et al. 2006, *ApJ*, in press (astro-ph/0606432)
- Peacock, J. A., Miller, L., & Longair, M. S. 1986, *MNRAS*, 218, 265
- Rayner, M. C. C. J. T. & Vacca, W. D. 2005, *ApJ*, 623, 1115
- Reid, I. N., Gizis, J. E., & Hawley, S. L. 2002, *AJ*, 124, 2721
- Richards, G. T. et al. 2006, *ApJS*, in press (astro-ph/0601558)
- Roellig, T. L. et al. 2004, *ApJS*, 154, 418
- Stern, D., Djorgovski, S. G., Perley, R., de Carvalho, R., & Wall, J. 2000, *AJ*, 132, 1526
- . 2005, *ApJ*, 631, 163
- Tyson, J. A. et al. 2005, *BAAS*, 207, #26.01
- Vrba, F. J. et al. 2004, *AJ*, 127, 2948
- Werner, M. W. et al. 2004, *ApJS*, 154, 1
- Wilson, A. S. & Colbert, E. J. M. 1995, *ApJ*, 438, 62
- Yan, H. et al. 2005, *ApJ*, 634, 109
- . 2006, *ApJ*, in press (astro-ph/0604554)

Table 1. Photometry of Boötes Field Candidates.

Target	B_W	R	I	J	K_s	[3.6]	[4.5]	[5.8]	[8.0]	Notes
ISS J142950.9+333012	> 27.1	> 26.1	22.12	16.88	16.99	15.76	15.04	15.05	14.56	T4.5 dwarf
ISS J142738.5+331242	> 27.1	> 26.1	22.03	19.83	18.17	16.57	15.92	15.28	14.81	$z = 6.12$
ISS J142729.6+352209	> 27.1	23.99	21.38	...	18.44	17.33	16.70	> 15.5	> 14.8	$z = 5.53$
ISS J142516.3+325409	> 27.1	23.76	21.15	17.41	16.77	> 15.5	> 14.8	$z = 5.85$

Note. — Photometry is all Vega-based, total magnitudes. Optical photometry is from NDWFS. Near-infrared photometry is from FLAMEX (Elston et al. 2006). Mid-infrared photometry is from the IRAC Shallow Survey (Eisenhardt et al. 2004). Non-detection limits are the average 5σ limits for the relevant bands across the entire field. Catalogued FLAMEX near-infrared photometry for the $z = 6.12$ quasar was corrupted by the bright, neighboring star. Photometry above comes instead from DAOPHOT analysis of the images, using stars in the field to model the PSF.